High-Fidelity Optical Readout of a Nuclear-Spin Qubit in Silicon Carbide

Erik Hesselmeier,[1,*] Pierre Kuna,[1,*] Wolfgang Knolle,[2] Florian Kaiser,[3,4] Nguyen Tien Son,[5] Misagh Ghezellou,[5] Jawad Ul-Hassan,[5] Vadim Vorobyov,[1,†] and Jörg Wrachtrup[1,6]

[1]*3rd Institute of Physics, IQST, and Research Center SCoPE, University of Stuttgart, Stuttgart, Germany*
[2]*Department of Sensoric Surfaces and Functional Interfaces, Leibniz-Institute of Surface Engineering (IOM), Leipzig, Germany*
[3]*Materials Research and Technology (MRT) Department, Luxembourg Institute of Science and Technology (LIST), 4422 Belvaux, Luxembourg*
[4]*University of Luxembourg, 41 rue du Brill, L-4422 Belvaux, Luxembourg*
[5]*Department of Physics, Chemistry and Biology, Linköping University, Linköping, Sweden*
[6]*Max Planck Institute for solid state physics, Stuttgart, Germany*

(Received 8 January 2024; accepted 10 April 2024; published 2 May 2024)

Quantum state readout is a key requirement for a successful qubit platform. In this work, we demonstrate a high-fidelity quantum state readout of a $V2$ center nuclear spin based on a repetitive readout technique. We demonstrate up to 99.5% readout fidelity and 99% for state preparation. Using this efficient readout, we initialize the nuclear spin by measurement and demonstrate its Rabi and Ramsey nutation. Finally, we use the nuclear spin as a long-lived memory for quantum sensing application of a weakly coupled diatomic nuclear-spin bath.

DOI: 10.1103/PhysRevLett.132.180804

Introduction.—Efficient readout of quantum states is at the heart of modern quantum technology. It allows one to perform single-shot measurements, i.e., the readout of the eigenstate of an individual quantum system reaching nearly unity fidelities [1–3]. Among numerous quantum technological platforms [4–6], optically active spin qubits [7] are one of the emerging solid state systems suitable for realization of optically interfaced spin registers [8]. Among them, the silicon vacancy ($V2$) center in 4H-SiC is an attractive solid state platform combining both excellent optical and host material properties. It possesses Fourier-limited optical transitions resilient to phonon broadening up to $T = 20$ K [9] and has tolerable optical coherence properties in nanophotonic structures [10,11], making it suitable for establishing an efficient spin-photon interface. Yet, low optical cyclicity and long-lived metastable states [12] have made a single-shot readout of a single-electron spin state impossible so far.

Achieving an efficient spin readout is a major milestone advancing various applications. High-fidelity optical readout of spin qubit states is important for quantum information processing, e.g., for feedback steps in error correction [13,14]. Additionally, a universal enhancement of the electron spin readout [15], as achieved here, boosts the sensitivity and speeds up the exploration of a rich nuclear-spin bath for Hamiltonian estimation of multispin registers [16]. An efficient spin readout also increases the success probability of high-fidelity heralded spin-photon entanglement, thus increasing its distribution rate. In the past, mapping of a short-lived electron spin state to a longer-lived one such as a charge state [17–20] or nuclear-spin states [21,22] was used to increase the signal to noise ratio beyond unity, required for single-shot readout. Additionally, an increase of the collection efficiency and emission rate of the emitted photons via photonic integration and the Purcell enhancement [23] has been used to improve the readout fidelity.

In this work, we perform a single-shot readout (SNR > 1) [24] of an ancillary neighboring ^{29}Si nuclear spin ($I = 1/2$) via repetitive mapping onto the electron spin state and optical readout. We analyze the stochastic switching dynamics of the nuclear spin under the readout and extract its main properties and use them to optimize the readout parameters. We find that state preparation fidelity of $\mathcal{F}_{\text{init}} = 99\%$ is achievable and a readout fidelity of $\mathcal{F}_{\text{read}} = 92\%$ in the case of no data loss. With postselection, we further boost the fidelity to $\mathcal{F}_{\text{read}} = 99.5\%$, albeit at a lower success rate of $\eta = 10\%$.

Furthermore, our model gives insights on the decay mechanisms of the memory. In particular, we see that the bright state decays tenfold faster, while the dark state is more stable under readout, which we use in the end for state preparation. Finally, we demonstrate the application of this readout for probing the coherence properties of the nuclear-spin memory and quantum sensing of weakly coupled nuclear spins. Our results mark a key achievement for the $V2$ system, bringing it closer to a fully fledged qubit platform.

Results.—For optical addressing, we use a single vacancy of silicon ($V2$ center) in the 4H-SiC crystal depicted in Fig. 1(a).

Its electron spin state can be probed by resonant optical excitation resulting in ≈0.02 photons per readout in our setup. This low photon rate and the fact that optical excitation resets the spin into the dark state prevents an

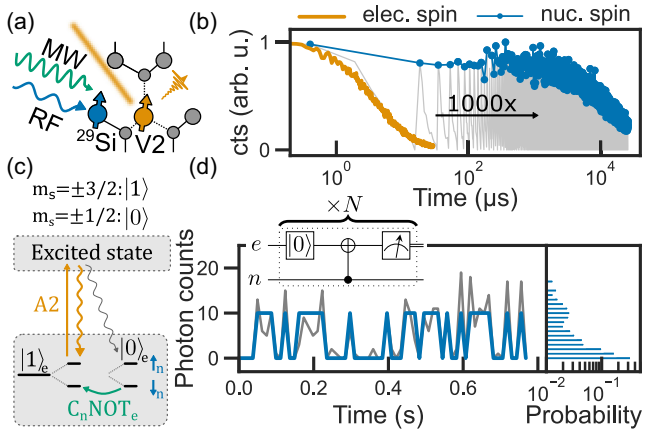

FIG. 1. (a) $V2$ center in 4H-SiC with nearby nuclear spin of ^{29}Si. (b) Photon emission under resonant excitation. Electron spin (orange) decays within a few microseconds, while the nuclear-spin state (blue) is preserved ≈1000 times longer. The gray line shows the restoration of the electron spin state and subsequent rise in photon collection. (c) During optical excitation, electron spin flips occur due to intersystem crossings. Population can be restored repeatedly via C_nNOT_e gates. $A2$ indicates the optical transition from $m_s \pm 3/2$ ground to excited state. (d) Real-time trace of nuclear-spin quantum jumps.

efficient electron state readout [orange curve in Fig. 1(b)]. Neighboring nuclear spins interact with the $V2$ electron spin density, giving rise to a hyperfine coupled electron-nuclear $S = 3/2 \otimes I = 1/2$ level system [Fig. 1(c)], and we utilize an electron qubit encoding as $|0\rangle = |\pm 1/2\rangle$, $|1\rangle = |\pm 3/2\rangle$.

For many of the nearby strongly coupled spins, the isotropic Fermi contact term results in an almost diagonal hyperfine tensor [25]. In analogy to the well-studied N-V system [21], at elevated magnetic fields B_z, the Hamiltonian of the system with aligned magnetic field reads

$$H_{g(e)} = D_{g(e)}\left(S_z^2 + \frac{1}{3}S(S+1)\right) + \gamma B_z S_z + A_{\perp}^{g(e)}(S_y I_y + S_x I_x) + A_{\parallel}^{g(e)} S_z I_z + \gamma_n B_z I_z, \quad (1)$$

where B is the applied magnetic field, S the spin operator of the electron, I the spin operator of the coupled nuclear spin, and $A_{\perp,\parallel}^{g(e)}$ the diagonal elements of the hyperfine tensor in ground (excited) state (see Table I). $D_{g(e)}$ is the zero field splitting in the ground (excited) state. At high magnetic fields, this Hamiltonian yields a robust nuclear qubit encoded in the eigenstates of the I_z operator. Its lifetime increases quadratically with the magnetic field [21] and allows one to probe the quantum state multiple times to overcome the shot noise of the optical readout. The prolonged T_1 time of the nuclear spin under readout condition compared to the electron spin is shown in Fig. 1(b). Hence, the spin states can be probed faster than spin flips occur as marked by the quantum jumps trajectory presented in Fig. 1(d). Here, we continuously probe the system and sum the collected photons of N subsequent reading steps to trace the spin quantum state. The count rate is directly related to the nuclear-spin state and enables observation of quantum jumps in real time. Each reading step contains a C_nNOT_e gate realized via two selective microwave π pulses $\pm 1/2 \rightarrow \pm 3/2$ conditional to the same nuclear-spin state and an electron state readout via $A2$ laser pulse. This laser pulse also resets the electron state into $m_s = \pm 1/2$ for the next iteration [gray line in Fig. 1(b)]. Throughout this Letter, $A1$ ($A2$) denotes the resonant laser transition between the ground and excited state of the $m_s = \pm 1/2$ ($m_s = \pm 3/2$) electron submanifold.

TABLE I. The ground state hyperfine tensor of the used nuclear spin. Units are in megahertz. A_{iso} is the Fermi contact interaction and T the dipolar interaction term.

A_{zz}	A_{xx}	A_{yy}	A_{iso}	T
8.660(3)	9.00(1)	9.03(1)	8.910(6)	−0.130(4)

To optimize the readout parameters, we first quantify the intrinsic switching and emission rates under the readout process analogous to [26]. In the first step, we exploit the two-point measurement scheme as described above with an additional charge-resonance check (CRC) to filter out individual ionization and off-resonance events [Fig. 2(a)]. CRC is performed by shining the $A1$ and $A2$ lasers simultaneously for 500 μs. In the case where both lasers are resonant to their respective optical transition and the defect is not ionized, the electron spin-independent excitation leads to emission of photons above a threshold of 2 [27]. This heralds the correct charge state of the defect.

We prepare the initial state by measurements, i.e., using a low count rate in first readout step ($R1$) (see below) as state indicator. By choosing the appropriate condition of the C_nNOT_e gate in the first readout, we prepare $m_i = |\uparrow\rangle$ or $m_i = |\downarrow\rangle$. We probe the nuclear-spin state with a second readout step ($R2$) and record a photon count distribution conditional on the state prepared by the first readout $m_i = |\uparrow(\downarrow)\rangle$ for various readout parameters. We depict the case of $N_1 = 400$, $N_2 = 300, 700$, $t_l = 15$ μs in Fig. 2(b), while other cases are presented in detail in [27]. By fitting the distribution with a numerical model [26], we extract switching (γ) and emission (λ) rates depending on the experimental parameters. For a readout time $t_l = 15$ μs and a laser power of 20 nW, we observe switching rates of $\gamma_0 = 8(2)$ Hz in the dark and $\gamma_1 = 100(10)$ Hz in the bright state. We attribute the fast decay rate from the bright state to the increased nuclear-spin flipping rates during the optical excitation cycle. The decay rate from the dark state is limited by the infidelity of nuclear state mapping to the electron state and an occasional unwanted excitation cycle,

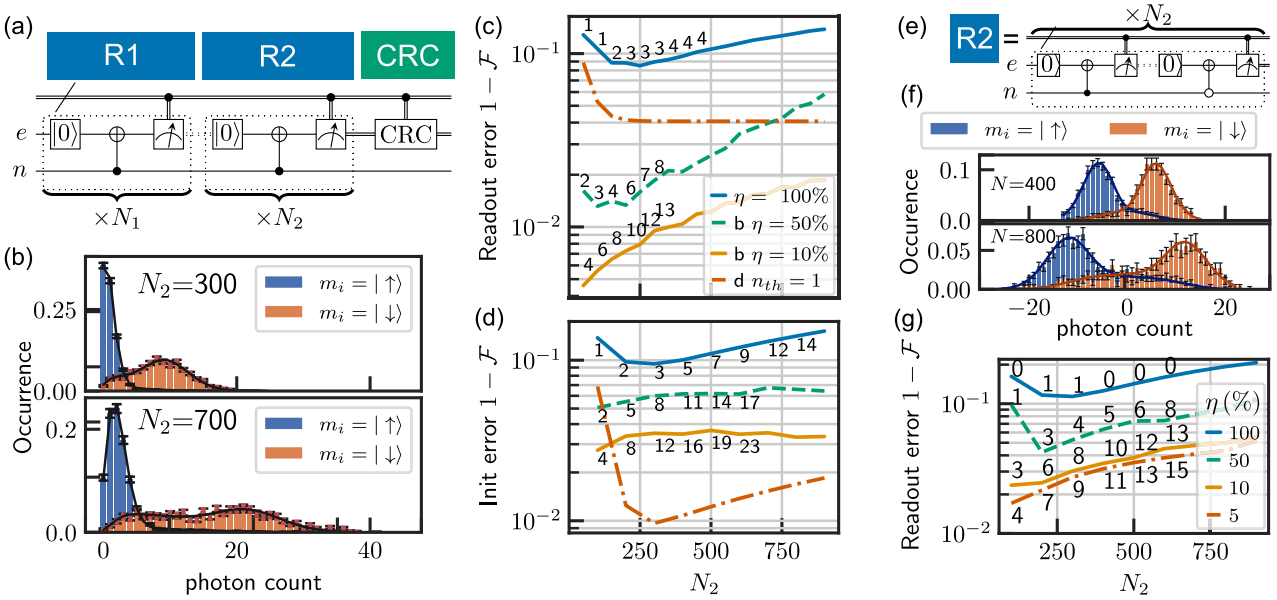

FIG. 2. (a) Two-point measurement scheme consisting of two readouts $R1$ and $R2$ and a CRC. (b) Photon count histogram for the second readout $R2$ conditioned on charge-resonance check and first readout $R1$. (c) Infidelity of the readout using the scheme described in (a). Numbers label the threshold photon count. η marks the success rate of the sequence. Legend is shared with (d). Blue, yellow, and green lines show initialization and readout fidelity of the bright state b. The red line indicates the fidelity of the dark state d. (d) Infidelity of state preparation by readout presented in (a). (e) Scheme for alternating addressing of both nuclear-spin states. (f) Distribution of difference of photon counts in alternating addressing of spin states. (g) Infidelity of readout of the scheme in (e).

which is supported by a much slower longitudinal spin relaxation in the absence of readout [27]. Next, using our experimentally calibrated switching model, we estimate the fidelity of the readout [Fig. 2(c)]. Using the maximum likelihood method [26], we estimate that with a success rate $\eta = 100\%$ of the readout an average fidelity for dark and bright states $\mathcal{F} = 92\%$ is achievable with $N_2 = 250$ repetitions and photon threshold of $n_{\mathrm{th}} = 3$. A better fidelity can be achieved by increasing the threshold for a bright state readout but has a limited effect on reading a dark state, due to the finite overlap of bright and dark distribution at $n = 0$ photon count. We see that a fidelity of 99.5% is achievable when increasing the threshold for reading the bright state, limited by a success rate $\eta = 10\%$ of the readout. For estimating the state preparation fidelity, we use the maximum likelihood method and photon count distribution conditioned on the state at the end of the readout as described in [26]. We find that conditioning to $n = 0$ photons prepares a dark state with fidelity of 99% at $N_1 = 300$, while preparation of the bright state with similar fidelity would be possible only when using even less than $\eta = 10\%$ success rate of the readout $R1$ and using higher threshold values. Thus, in our work, we use the dark state preparation, which combined with CRC heralds a high fidelity of dark nuclear-spin state.

The readout method with probing only one bright state has a limited overall fidelity, since the dark state readout fidelity could not be improved by a stronger postselection and sacrificing of the success rate. Spin-state-independent

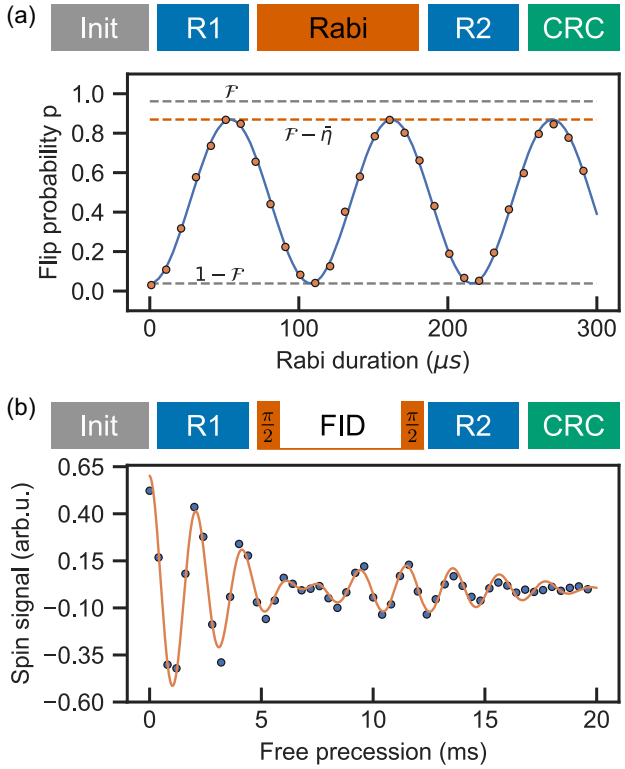

FIG. 3. Coherent control of the nuclear-spin qubit. (a) Measurement of the nuclear Rabi nutations via initialization, readout 1 ($R1$), Rabi drive for various durations, and readout 2 ($R2$), followed by CRC. (b) Free precession (Ramsey) of the nuclear spin.

high-fidelity readout can be achieved when using alternating addressing of both nuclear-spin states and in the end comparing the two accumulated count rates $n = n_1 - n_2$ [Fig. 2(e)]. In this case, both nuclear-spin states are bright and allow postselection with higher thresholds [Fig. 2(f)]. We use a switching model based on Skellam distribution [27] adapted from [26] to extract the rates and find that in this case the switching rates are half of those for the bright states for both states, resulting from the fact that both states are probed 50% of the overall readout time. The numerical analysis shows that one can achieve $\mathcal{F} = 98\%$ fidelity for average fidelity of both states with $\eta = 5\%$–10% success rate [Fig. 2(g)]. This can be further improved by reducing the success rate, showing that there is a trade-off relation.

We further measure Rabi oscillations of the nuclear spins [Fig. 3(a)]. For this, we exploit the two-point measurement scheme as explained before and flip the nuclear spin in both states $m_s = \pm 1/2$ with the same Rabi frequency. We observe a high nuclear-spin contrast, which corresponds to fidelity of $\mathcal{F} = 96\%$ for readout with about $\eta = 90\%$ success rate. Furthermore, we perform a nuclear-spin Ramsey measurement in electron subdomain $m_s = +1/2$ and obtain $T_2^* = 7.7(7)$ ms [Fig. 3(b)], a higher value than previously measured at smaller B fields [25]. We note an additional beating oscillation, presumably originating from additional coupling to another nuclear spin. This could enable utilization of stronger coupled nuclear spins to address the weaker coupled and obtain nuclear-nuclear J coupling, required for full system Hamiltonian estimation.

Finally, we apply the efficient readout for probing the weakly coupled nuclear spins (Fig. 4). We use an electron-nuclear double-resonance (ENDOR) pulse sequence [28] for probing the A_{zz} coupled nuclear spins, where the nuclear spin is used as memory and a readout ancillary spin and the electron spin as a sensor. The sequence exploits the electron-nuclear double-resonance condition and results in a readout contrast increase, once the target spins are flipped. We scan the frequency of the probing pulse and observe two distinct location of peaks centered at the positions of the expected Larmor frequency of corresponding nuclear-spin baths of ^{29}Si and ^{13}C. We observe eight individual peaks around ^{29}Si bath and four individual peaks around ^{13}C bath with coupling strength within the 10–100 kHz range, suitable for utilizing as building blocks of a quantum register.

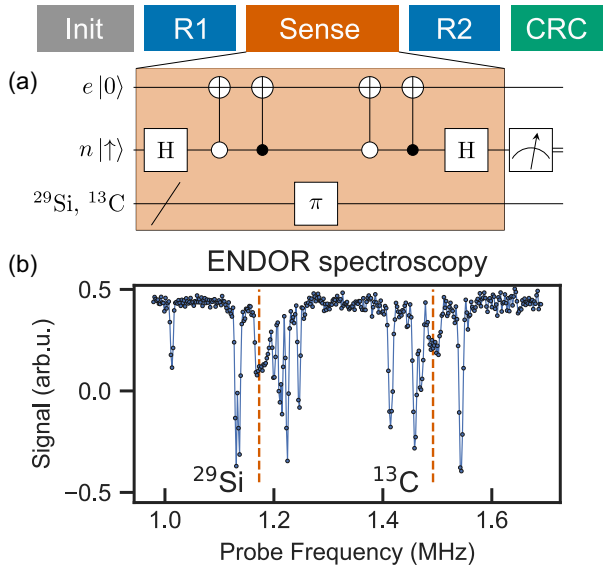

FIG. 4. ENDOR spectroscopy of nuclear-spin bath. (a) Measurement protocol. Initialization and readout are performed similarly to as in Fig. 3. The coherent control is performed via entanglement of nuclear and electron spin. This state acquires a phase conditioned on whether the target nuclear spins are probed with a resonant microwave π pulse. (b) ENDOR spectra of nuclear-spin bath containing ^{13}C and ^{29}Si spins. Vertical dashed lines mark the expected Larmor frequency based on the estimated B field.

Conclusion.—In this work, we show high-fidelity readout of a single nuclear spin around $V2$ center with fidelity reaching 99.5%. We demonstrate that such readout can serve for initialization by measurement with fidelity reaching 99%. We show coherent control of the nuclear spin after initialization by measurement and demonstrate the application of the high-fidelity readout for the efficient sensing of weakly coupled nuclear spins. A further improvement in fidelity could be reached by further increasing the B field values, as the lifetime of the spin increases quadratically with the B field [21]. Furthermore, the integration of $V2$ centers into photonic nanostructures would allow one to increase the number of detected photons per iteration, which can boost success rates and allow for higher fidelities at lower magnetic fields. Weaker coupled nuclear spins [29] will favor higher fidelities at smaller magnetic fields as well. Our results mark the important step forward for the qubit candidate system $V2$ center in 4H-SiC, i.e., single-shot readout, important for quantum information applications such as quantum information processing, state preparation by measurement, and quantum sensing. We acknowledge similar work performed by Lai *et al.* [30].

P. K., F. K., J. U.-H., and J. W. acknowledge support from the European Commission through the QuantERA project InQuRe (Grant Agreements No. 731473 and No. 101017733). P. K., F. K., and J. W. acknowledge the German ministry of education and research for the project InQuRe (BMBF, Grant Agreement No. 16KIS1639K). F. K. and J. W. acknowledge support from the European Commission for the Quantum Technology Flagship project QIA (Grant Agreements No. 101080128 and No. 101102140), the German ministry of education and research for the project QR.X (BMBF, Grant Agreement No. 16KISQ013), and Baden-Württemberg Stiftung for the project SPOC (Grant Agreement No. QT-6). J. W. also

acknowledges support from the project Spinning (BMBF, Grant Agreement No. 13N16219) and the German Research Foundation (DFG, Grant Agreement No. GRK2642). J. U.-H. further acknowledges support from the Swedish Research Council under VR Grant No. 2020-05444 and Knut and Alice Wallenberg Foundation (Grant No. KAW 2018.0071).

Appendix A: Experimental setup.—All experiments were performed at cryogenic temperature < 10 K in a Montana Instruments cryostation. A self-built confocal microscope was used to optically excite single $V2$ centers and detect the redshifted phonon sideband. Initialization of the charge state is performed by off-resonant excitation via a 728 nm diode laser (Toptica iBeam Smart). For resonant optical excitation, we used an external cavity tunable diode laser (Toptica DL Pro), which was split and frequency shifted by two separate acousto-optic modulators to address both optical transitions selectively. Those transitions are called $A1$ and $A2$ and are split by ≈ 1 GHz, depending on the zero field splitting of the excited state. Laser photons are filtered by two tunable long-pass filters (Semrock TLP01-995). The magnetic field is created via a electromagnet from GWM Associates (Model No. 5403EG-50) connected to a power supply from Danfysik (SYSTEM 8500 magnet power supply). In this work, a magnetic field of $B \sim 0.14$ T was used. If not indicated otherwise, we used 20 nW $A2$ excitation power before the cryostation. The used detectors are fiber-coupled superconducting nanowire single-photon detectors from Photon Spot.

Appendix B: Silicon carbide sample.—The used substrate has a natural abundance of silicon (4.7% ^{29}Si) and carbon (1.1% ^{13}C) isotopes, which are spin $I = 1/2$ nuclei.

*These authors contributed equally to this letter.
†v.vorobyov@pi3.uni-stuttgart.de

[1] A. H. Myerson, D. J. Szwer, S. C. Webster, D. T. C. Allcock, M. J. Curtis, G. Imreh, J. A. Sherman, D. N. Stacey, A. M. Steane, and D. M. Lucas, High-fidelity readout of trapped-ion qubits, Phys. Rev. Lett. **100**, 200502 (2008).
[2] T. Walter, P. Kurpiers, S. Gasparinetti, P. Magnard, A. Potočnik, Y. Salathé, M. Pechal, M. Mondal, M. Oppliger, C. Eichler, and A. Wallraff, Rapid high-fidelity single-shot dispersive readout of superconducting qubits, Phys. Rev. Appl. **7**, 054020 (2017).
[3] J. J. Pla, K. Y. Tan, J. P. Dehollain, W. H. Lim, J. J. L. Morton, F. A. Zwanenburg, D. N. Jamieson, A. S. Dzurak, and A. Morello, High-fidelity readout and control of a nuclear spin qubit in silicon, Nature (London) **496**, 334 (2013).
[4] M. H. Devoret and R. J. Schoelkopf, Superconducting circuits for quantum information: An outlook, Science **339**, 1169 (2013).
[5] M. Saffman, T. G. Walker, and K. Mølmer, Quantum information with Rydberg atoms, Rev. Mod. Phys. **82**, 2313 (2010).
[6] D. Wineland and D. Leibfried, Quantum information processing and metrology with trapped ions, Laser Phys. Lett. **8**, 175 (2011).
[7] D. D. Awschalom, R. Hanson, J. Wrachtrup, and B. B. Zhou, Quantum technologies with optically interfaced solid-state spins, Nat. Photonics **12**, 516 (2018).
[8] N. Kalb, A. A. Reiserer, P. C. Humphreys, J. J. W. Bakermans, S. J. Kamerling, N. H. Nickerson, S. C. Benjamin, D. J. Twitchen, M. Markham, and R. Hanson, Entanglement distillation between solid-state quantum network nodes, Science **356**, 928 (2017).
[9] P. Udvarhelyi, G. m. H. Thiering, N. Morioka, C. Babin, F. Kaiser, D. Lukin, T. Ohshima, J. Ul-Hassan, N. T. Son, J. Vučković, J. Wrachtrup, and A. Gali, Vibronic states and their effect on the temperature and strain dependence of silicon-vacancy qubits in 4H-SiC, Phys. Rev. Appl. **13**, 054017 (2020).
[10] C. Babin *et al.*, Fabrication and nanophotonic waveguide integration of silicon carbide colour centres with preserved spin-optical coherence, Nat. Mater. **21**, 67 (2022).
[11] D. M. Lukin, M. A. Guidry, J. Yang, M. Ghezellou, S. Deb Mishra, H. Abe, T. Ohshima, J. Ul-Hassan, and J. Vučković, Two-emitter multimode cavity quantum electrodynamics in thin-film silicon carbide photonics, Phys. Rev. X **13**, 011005 (2023).
[12] D. Liu, F. Kaiser, V. Bushmakin, E. Hesselmeier, T. Steidl, T. Ohshima, N. T. Son, J. Ul-Hassan, Ö. O. Soykal, and J. Wrachtrup, The silicon vacancy centers in SiC: Determination of intrinsic spin dynamics for integrated quantum photonics, arXiv:2307.13648.
[13] G. Waldherr, Y. Wang, S. Zaiser, M. Jamali, T. Schulte-Herbrüggen, H. Abe, T. Ohshima, J. Isoya, J. Du, P. Neumann, and J. Wrachtrup, Quantum error correction in a solid-state hybrid spin register, Nature (London) **506**, 204 (2014).
[14] J. Cramer, N. Kalb, M. A. Rol, B. Hensen, M. S. Blok, M. Markham, D. J. Twitchen, R. Hanson, and T. H. Taminiau, Repeated quantum error correction on a continuously encoded qubit by real-time feedback, Nat. Commun. **7**, 11526 (2016).
[15] M. Steiner, P. Neumann, J. Beck, F. Jelezko, and J. Wrachtrup, Universal enhancement of the optical readout fidelity of single electron spins at nitrogen-vacancy centers in diamond, Phys. Rev. B **81**, 035205 (2010).
[16] M. H. Abobeih, J. Randall, C. E. Bradley, H. P. Bartling, M. A. Bakker, M. J. Degen, M. Markham, D. J. Twitchen, and T. H. Taminiau, Atomic-scale imaging of a 27-nuclear-spin cluster using a quantum sensor, Nature (London) **576**, 411 (2019).
[17] J. M. Elzerman, R. Hanson, L. H. Willems van Beveren, B. Witkamp, L. M. K. Vandersypen, and L. P. Kouwenhoven, Single-shot read-out of an individual electron spin in a quantum dot, Nature (London) **430**, 431 (2004).
[18] R. Hanson, L. Willems van Beveren, I. Vink, J. Elzerman, F. Koppens, L. Kouwenhoven, and L. Vandersypen, Single-shot readout of electron spins in a semiconductor quantum dot, Physica (Amsterdam) **34E**, 1 (2006).

[19] B. J. Shields, Q. P. Unterreithmeier, N. P. de Leon, H. Park, and M. D. Lukin, Efficient readout of a single spin state in diamond via spin-to-charge conversion, Phys. Rev. Lett. **114**, 136402 (2015).

[20] C. P. Anderson, E. O. Glen, C. Zeledon, A. Bourassa, Y. Jin, Y. Zhu, C. Vorwerk, A. L. Crook, H. Abe, J. Ul-Hassan, T. Ohshina, N. T. Son, G. Galli, and D. D. Awschalom, Five-second coherence of a single spin with single-shot readout in silicon carbide, Sci. Adv. **8**, abm5912 (2022).

[21] P. Neumann, J. Beck, M. Steiner, F. Rempp, H. Fedder, P. R. Hemmer, J. Wrachtrup, and F. Jelezko, Single-shot readout of a single nuclear spin, Science **329**, 542 (2010).

[22] A. Dréau, P. Spinicelli, J. R. Maze, J.-F. Roch, and V. Jacques, Single-shot readout of multiple nuclear spin qubits in diamond under ambient conditions, Phys. Rev. Lett. **110**, 060502 (2013).

[23] D. M. Lukin, M. A. Guidry, and J. Vučković, Integrated quantum photonics with silicon carbide: Challenges and prospects, PRX Quantum **1**, 020102 (2020).

[24] D. A. Hopper, H. J. Shulevitz, and L. C. Bassett, Spin readout techniques of the nitrogen-vacancy center in diamond, Micromachines **9**, 437 (2018).

[25] E. Hesselmeier, P. Kuna, I. Takács, V. Ivády, W. Knolle, N. T. Son, M. Ghezellou, J. Ul-Hassan, D. Dasari, F. Kaiser *et al.*, Qudit-based spectroscopy for measurement and control of nuclear-spin qubits in silicon carbide, Phys. Rev. Lett. **132**, 090601 (2024).

[26] M. Zahedian, M. Keller, M. Kwon, J. Javadzade, J. Meinel, V. Vorobyov, and J. Wrachtrup, On readout and initialisation fidelity by finite demolition single shot readout, Quantum Sci. Technol. **9**, 015023 (2023).

[27] See Supplemental Material at http://link.aps.org/supplemental/10.1103/PhysRevLett.132.180804, which includes Ref. [26], for additional information about the experimental method.

[28] N. Aslam, M. Pfender, P. Neumann, R. Reuter, A. Zappe, F. Fávaro de Oliveira, A. Denisenko, H. Sumiya, S. Onoda, J. Isoya, and J. Wrachtrup, Nanoscale nuclear magnetic resonance with chemical resolution, Science **357**, 67 (2017).

[29] A. P. Nizovtsev, S. Y. Kilin, A. L. Pushkarchuk, V. A. Pushkarchuk, S. A. Kuten, O. A. Zhikol, S. Schmitt, T. Unden, and F. Jelezko, Non-flipping ^{13}C spins near an NV center in diamond: Hyperfine and spatial characteristics by density functional theory simulation of the $C_{510}[NV]H_{252}$ cluster, New J. Phys. **20**, 023022 (2018).

[30] X.-Y. Lai, R.-Z. Fang, T. Li, R.-Z. Su, J. Huang, H. Li, L.-X. You, X.-H. Bao, and J.-W. Pan, preceding Letter, Single-shot readout of a nuclear spin in silicon carbide, Phys. Rev. Lett. **132**, 180803 (2024).